

Spin polarizations under a pseudovector interaction between quarks with the Kobayashi-Maskawa-'t Hooft term in high density quark matter

Masatoshi MORIMOTO¹, Yasuhiko TSUE², João da PROVIDÊNCIA³,
Constança PROVIDÊNCIA³ and Masatoshi YAMAMURA⁴

¹*Graduate School of Integrated Arts and Science, Kochi University, Kochi 780-8520, Japan*

²*Department of Mathematics and Physics, Kochi University, Kochi 780-8520, Japan*

³*CFisUC, Departamento de Física, Universidade de Coimbra, 3004-516 Coimbra, Portugal*

⁴*Department of Pure and Applied Physics, Faculty of Engineering Science, Kansai University, Suita 564-8680, Japan*

A possibility of a quark spin polarization originated from a pseudovector condensate is investigated in the three-flavor Nambu-Jona-Lasinio model with the Kobayashi-Maskawa-'t Hooft interaction which leads to flavor mixing. It is shown that a pseudovector condensate related to the strange quark easily occurs compared with pseudovector condensate related to light quarks. Further, it is shown that the pseudovector condensate related to the strange quark appears at a slightly small chemical potential by the effect of the flavor mixing due to the Kobayashi-Maskawa-'t Hooft interaction.

§1. Introduction

One of recent interests in many-particle systems governed by quantum chromodynamics (QCD) is to clarify the existence of various phases in high density and finite or zero temperature quark matter.¹⁾ Especially, in quark matter at finite density and low temperature, there may exist various phases such as the color superconducting phase,^{2)–4)} the quarkyonic phase,⁵⁾ the inhomogeneous chiral condensed phase,⁶⁾ the quark ferromagnetic phase,⁷⁾ the color-ferromagnetic phase,⁸⁾ the spin polarized phase due to the axial vector interaction^{9),10)} or due to the tensor interaction^{11)–21)} and so forth. In order to investigate the phase structure in quark matter, various effective models of QCD are used because in the region with low temperature and high density, namely large quark chemical potential, the numerical simulation by using the lattice QCD did not work until now, while in the region of high temperature and zero density, the lattice QCD simulation gives useful information about the phase structure.

As one of the effective models of QCD, the Nambu-Jona-Lasinio (NJL) model²²⁾ is widely used^{23),24)} because the NJL model has an important chiral symmetry of QCD. This model is used to investigate quark matter in the region with large quark chemical potential at low temperature.²⁵⁾ Thus, the physics related to the chiral symmetry or chiral symmetry breaking is well described. By using the extended NJL model in which the tensor-type four-point interaction and/or the vector-

pseudovector-type four-point interaction between quarks is introduced retaining the chiral symmetry, the possibility of the tensor condensate and/or pseudovector condensate has been investigated.^{11)–16), 19)–21), 26)} Since it has been shown that the quark spin polarization leads to the spontaneous magnetization in quark matter in the case of tensor-type¹⁶⁾ or pseudovector-type interaction²⁷⁾ between quarks in the NJL model, there exists a possibility that it gives origin to the strong magnetic field of compact stars such as neutron stars and magnetars.²⁸⁾

In this paper, we concentrate on the spin polarization due to the pseudovector condensate originated from the pseudovector interaction between quarks in an extended NJL model. In our previous paper in 27), the spin polarization due to the pseudovector condensate has been investigated in the case of the two-flavor NJL model. Then, it has been shown that the pseudovector condensate appears in a rather narrow region of the quark chemical potential just before the chiral symmetry is restored. In this region, the dynamical quark mass is still not zero. However, if quark mass becomes zero, the pseudovector condensate disappears even if the strength of pseudovector interaction is very large. Thus, there may be a possibility of the existence of the pseudovector condensate related to the strange quark because the strange quark has a finite current quark mass even in the region with large quark chemical potential, namely high density. Because the pseudovector condensate leads to spin polarization and spontaneous magnetization, it is interesting to investigate a possibility of the pseudovector condensate in the three-flavor NJL model. In three-flavor case, it is well known that the quark-flavor mixing occurs through the six-point interaction between quarks in the NJL model. This interaction is called the Kobayashi-Maskawa-'t Hooft interaction or the determinant interaction.^{29), 30)} Thus, in this paper, the effect of the flavor mixing on the appearance of pseudovector condensate is also investigated.

This paper is organized as follows: In the next section, the mean field approximation for the NJL model with vector-pseudovector-type four-point interaction between quarks is given. Then, both the quark and antiquark condensate, namely chiral condensate, and the pseudovector condensate, namely spin polarization, are introduced and in section 3, the thermodynamic potential is evaluated at zero temperature with finite quark chemical potential. Both the condensates are treated self-consistently by means of the gap equations. In section 4, the solutions of the gap equations are numerically given and the behaviors of the pseudovector condensates and the dynamical quark masses related to the light quarks (u and d quarks) and the strange quark are investigated. The last section is devoted to a summary and concluding remarks.

§2. Mean field approximation for the Nambu-Jona-Lasinio model with vector-pseudovector-type four-point interaction between quarks

Let us start from the three-flavor Nambu-Jona-Lasinio model with vector-pseudovector-type^{9), 10)} four-point interactions between quarks. The Lagrangian density can be

expressed as

$$\begin{aligned}
\mathcal{L} &= \mathcal{L}_0 + \mathcal{L}_m + \mathcal{L}_S + \mathcal{L}_P + \mathcal{L}_D, \\
\mathcal{L}_0 &= \bar{\psi} i \gamma^\mu \partial_\mu \psi, \\
\mathcal{L}_m &= -\bar{\psi} \vec{m}_0 \psi, \\
\mathcal{L}_S &= \frac{G_s}{2} \sum_{a=0}^8 [(\bar{\psi} \lambda_a \psi)^2 + (\bar{\psi} i \lambda_a \gamma_5 \psi)^2], \\
\mathcal{L}_P &= -\frac{G_p}{2} \sum_{a=0}^8 [(\bar{\psi} \gamma^\mu \lambda_a \psi)^2 + (\bar{\psi} i \gamma_5 \gamma^\mu \lambda_a \psi)^2], \\
\mathcal{L}_D &= G_D [\det \bar{\psi} (1 - \gamma_5) \psi + \det \bar{\psi} (1 + \gamma_5) \psi], \tag{2.1}
\end{aligned}$$

where \vec{m}_0 represents a current quark mass matrix in flavor space as follows :

$$\vec{m}_0 = \text{diag} (m_u, m_d, m_s) . \tag{2.2}$$

Here, \mathcal{L}_P represents a four-point vector and pseudovector interaction between quarks in the three-flavor case which preserves chiral symmetry. Also, \mathcal{L}_D represents so-called the Kobayashi-Maskawa-'t Hooft or the determinant interaction term which leads to the six-point interaction between quarks in the three-flavor case.

Hereafter, we treat the above model within the mean field approximation. First, we ignore non-diagonal components of the condensates in a flavor space. Therefore, terms in a summation of Gell-Mann matrices are restricted to the diagonal entries with $a = 0, 3$ and 8 :

$$\begin{aligned}
\sum_{a=0}^8 [(\bar{\psi} \lambda_a \Gamma \psi)^2] &\longrightarrow \sum_{a=0,3,8} [(\bar{\psi} \lambda_a \Gamma \psi)^2] \\
&= \frac{2}{3} [(\bar{u} \Gamma u + \bar{d} \Gamma d + \bar{s} \Gamma s)]^2 + [(\bar{u} \Gamma u - \bar{d} \Gamma d)]^2 \\
&\quad + \frac{1}{3} [(\bar{u} \Gamma u + \bar{d} \Gamma d - 2\bar{s} \Gamma s)]^2 \\
&= 2(\bar{u} \Gamma u)^2 + 2(\bar{d} \Gamma d)^2 + 2(\bar{s} \Gamma s)^2 . \tag{2.3}
\end{aligned}$$

Here, Γ means products of any gamma matrices or unit matrix. Also, in the determinant interaction term, \mathcal{L}_D , the same approximation is adopted, namely, the off-diagonal matrix elements in the flavor space are omitted:

$$\begin{aligned}
&\det \bar{\psi} (1 - \gamma_5) \psi + \det \bar{\psi} (1 + \gamma_5) \psi \\
&\longrightarrow \det \begin{pmatrix} \bar{u}(1 - \gamma_5)u & 0 & 0 \\ 0 & \bar{d}(1 - \gamma_5)d & 0 \\ 0 & 0 & \bar{s}(1 - \gamma_5)s \end{pmatrix} \\
&\quad + \det \begin{pmatrix} \bar{u}(1 + \gamma_5)u & 0 & 0 \\ 0 & \bar{d}(1 + \gamma_5)d & 0 \\ 0 & 0 & \bar{s}(1 + \gamma_5)s \end{pmatrix}
\end{aligned}$$

$$\begin{aligned}
&= 2(\bar{u}u)(\bar{d}d)(\bar{s}s) \\
&\quad + 2(\bar{u}u)(\bar{d}\gamma_5 d)(\bar{s}\gamma_5 s) + 2(\bar{u}\gamma_5 u)(\bar{d}d)(\bar{s}\gamma_5 s) + 2(\bar{u}\gamma_5 u)(\bar{d}\gamma_5 d)(\bar{s}s) .
\end{aligned} \tag{2.4}$$

Secondly, in order to consider the spin polarization under the mean field approximation, the pseudovector condensate $\langle \bar{q}\gamma_5\gamma^3 q \rangle = \langle q^\dagger \Sigma_3 q \rangle$ is taken into account as well as the chiral condensate $\langle \bar{q}q \rangle$. It should be noted that the pseudovector condensate for $\langle \bar{q}\gamma_5\gamma^\nu q \rangle$ with $\nu = 3$ is nothing but the expectation value of the spin matrix Σ_3 for the quark number density $q^\dagger q$. Thus, the pseudovector condensate $\langle \bar{q}\gamma_5\gamma^3 q \rangle$ can be regarded as a quark spin polarization. Then, the Lagrangian density (2.1) reduces to

$$\begin{aligned}
\mathcal{L}_{MF} = & \bar{\psi}(i\gamma^\mu \partial_\mu - \vec{M}_q)\psi - \vec{U}\psi^\dagger \Sigma_3 \psi \\
& - \sum_f \left(\frac{M(f)^2}{4G_s} + \frac{U_f^2}{4G_p} \right) + \frac{1}{2} \frac{G_D}{G_s^3} M(u)M(d)M(s) ,
\end{aligned} \tag{2.5}$$

where $f = u, d$ or s and

$$\begin{aligned}
\Sigma_3 &= -\gamma^0 \gamma_5 \gamma^3 = \begin{pmatrix} \sigma_3 & 0 \\ 0 & \sigma_3 \end{pmatrix} \\
\vec{M}_q &= \text{diag.} \left(m_u + M(u) - \frac{G_D}{2G_s^2} M(d)M(s) , m_d + M(d) - \frac{G_D}{2G_s^2} M(s)M(u) , \right. \\
&\quad \left. m_s + M(s) - \frac{G_D}{2G_s^2} M(u)M(d) \right) \\
&= \text{diag.}(M_u, M_d, M_s) \\
M(f) &= -2G_s \langle \bar{q}_f q_f \rangle
\end{aligned} \tag{2.6}$$

$$\begin{aligned}
\vec{U} &= \text{diag.}(U_u, U_d, U_s) \\
U_f &= -2G_p \langle q_f^\dagger \Sigma_3 q_f \rangle .
\end{aligned} \tag{2.7}$$

Here, σ_3 is the third component of the Pauli spin matrices.

Introducing the quark chemical potential μ in order to consider a quark matter at finite density, the Hamiltonian density can be obtained from the Lagrangian density as

$$\begin{aligned}
\mathcal{H}_{MF} - \mu \mathcal{N} = & \bar{\psi} \left(-i\boldsymbol{\gamma} \cdot \boldsymbol{\nabla} + \vec{M}_q - \mu \gamma^0 + \vec{U} \gamma^0 \Sigma_3 \right) \psi \\
& + \sum_f \left(\frac{M(f)^2}{4G_s} + \frac{U_f^2}{4G_p} \right) - \frac{1}{2} \frac{G_D}{G_s^3} M(u)M(d)M(s) ,
\end{aligned} \tag{2.8}$$

where \mathcal{N} represents the quark number density, $\psi^\dagger \psi$.

§3. Thermodynamic potential

In this section, let us derive the effective potential or the thermodynamic potential at zero temperature. The Hamiltonian density (2.8) can be rewritten as

$$\mathcal{H}_{MF} - \mu\mathcal{N} = \psi^\dagger(h_A - \mu)\psi + \sum_f \left(\frac{M(f)^2}{4G_s} + \frac{U_f^2}{4G_p} \right) - \frac{1}{2} \frac{G_D}{G_s^3} M(u)M(d)M(s) \quad (3.9)$$

$$h_A = -i\gamma^0 \boldsymbol{\gamma} \cdot \boldsymbol{\nabla} + \gamma^0 \vec{M}_q + \vec{U} \Sigma_3. \quad (3.10)$$

In order to obtain the eigenvalues of the single-particle Hamiltonian h_A , namely the energy eigenvalues of single quark, it is necessary to diagonalize h_A , the eigenvalues of which can be obtained easily as

$$E_{p_x, p_y, p_z, \eta}^f = \sqrt{p_x^2 + p_y^2 + \left(\sqrt{p_z^2 + M_f^2} + \eta U_f \right)^2}, \quad (3.11)$$

where $\eta = \pm 1$. Thus, we can easily evaluate the thermodynamic potential with the above single-particle energy eigenvalues. Then, the thermodynamic potential Φ can be expressed as

$$\begin{aligned} \Phi = & \sum_{f, \alpha, \eta} \int \frac{dp_z}{2\pi} \int \frac{dp_x}{2\pi} \int \frac{dp_y}{2\pi} \left(E_{p_x, p_y, p_z, \eta}^f - \mu \right) \theta \left(\mu - E_{p_x, p_y, p_z, \eta}^f \right) \\ & - \sum_{f, \alpha, \eta} \int \frac{dp_z}{2\pi} \int \frac{dp_x}{2\pi} \int \frac{dp_y}{2\pi} E_{p_x, p_y, p_z, \eta}^f \\ & + \sum_f \left(\frac{M(f)^2}{4G_s} + \frac{U_f^2}{4G_p} \right) + \frac{1}{2} \frac{G_D}{G_s^3} M(u)M(d)M(s). \end{aligned} \quad (3.12)$$

Here, $\theta(x)$ represents the Heaviside step function. The first and second lines in (3.12) represent the positive-energy contribution of quarks and the vacuum contribution, respectively. To make the calculation easier, we substitute $p_x^2 + p_y^2 \equiv p_\perp^2$. Then, the energy eigenvalues and the thermodynamic potential are rewritten as

$$\begin{aligned} E_{p_x, p_y, p_z, \eta}^f &= \sqrt{p_\perp^2 + \left(\sqrt{p_z^2 + M_{qf}^2} + \eta U_f \right)^2} \\ &\equiv E_{p_\perp, p_z, \eta}^f, \end{aligned} \quad (3.13)$$

$$\begin{aligned} \Phi = & \sum_{f, \alpha, \eta} \int \frac{dp_z}{2\pi} \int \frac{dp_\perp}{2\pi} p_\perp \left(E_{p_\perp, p_z, \eta}^f - \mu \right) \theta \left(\mu - E_{p_\perp, p_z, \eta}^f \right) \\ & - \sum_{f, \alpha, \eta} \int \frac{dp_z}{2\pi} \int \frac{dp_\perp}{2\pi} p_\perp E_{p_\perp, p_z, \eta}^f \\ & + \sum_f \left(\frac{M(f)^2}{4G_s} + \frac{U_f^2}{4G_p} \right) + \frac{1}{2} \frac{G_D}{G_s^3} M(u)M(d)M(s). \end{aligned} \quad (3.14)$$

Noting the condition $(\mu > E_{p_\perp, p_z, \eta}^f)$ due to the step function, integration ranges of positive-energy contribution should be carefully estimated. First of all,

$$0 \leq p_\perp \leq \sqrt{\mu^2 - \left(\sqrt{p_z^2 + M_q^2} + \eta U\right)^2} \quad (3.15)$$

should be satisfied. Next, for the $\eta = +1$ case, integration range of p_z is

$$|p_z| \leq \sqrt{(\mu - U)^2 - M_q^2} \quad (3.16)$$

because p_\perp is real. On the other hand, for $\eta = -1$ case, the followings are obtained:

$$\left\{ \begin{array}{l} \text{for } U \leq M_q \cdots |p_z| \leq \sqrt{(\mu + U)^2 - M_q^2} \\ \text{for } M_q \leq U \cdots \left\{ \begin{array}{l} \text{for } \mu \leq U \cdots \sqrt{(U - \mu)^2 - M_q^2} \leq |p_z| \leq \sqrt{(U + \mu)^2 - M_q^2} \\ \text{for } U \leq \mu \cdots |p_z| \leq \sqrt{(U + \mu)^2 - M_q^2} \end{array} \right. \end{array} \right. \quad (3.17)$$

As for the vacuum contributions, since the NJL model is not a renormalizable model, the three-momentum cutoff Λ is usually introduced as

$$p_x^2 + p_y^2 + p_z^2 \leq \Lambda^2. \quad (3.18)$$

Thus, the thermodynamic potential (3.12) can be divided into two parts and can be evaluated as follows :

$$\Phi = \Phi_\mu + \Phi_{vac}, \quad (3.19)$$

$$\begin{aligned} \Phi_\mu = & \frac{3}{2\pi^2} \sum_f \left[\frac{p_z}{24} (12U\mu - 12U^2 - 5M_q - 2p_z^2) \sqrt{M_q^2 + p_z^2} + 4p_z^3 (\mu - 2U) \right. \\ & - p_z (24M_q^2 U + 12M_q^2 \mu - 8U^3 + 12U^2 \mu - 4\mu^3) \\ & \left. - \frac{1}{8} M_q^2 (M_q^2 + 4U^2 - 4U\mu) \ln \left(p_z + \sqrt{M_q^2 + p_z^2} \right) \right]_{0}^{p_{Max}} \\ & + \frac{3}{2\pi^2} \sum_f \left[-\frac{p_z}{24} (12U\mu + 12U^2 + 5M_q + 2p_z^2) \sqrt{M_q^2 + p_z^2} + 4p_z^3 (\mu + 2U) \right. \\ & - p_z (-24M_q^2 U + 12M_q^2 \mu + 8U^3 + 12U^2 \mu - 4\mu^3) \\ & \left. - \frac{1}{8} M_q^2 (M_q^2 + 4U^2 + 4U\mu) \ln \left(p_z + \sqrt{M_q^2 + p_z^2} \right) \right]_{p_{min}}^{p_{Max}}, \quad (3.20) \end{aligned}$$

$$\Phi_{vac} = \frac{1}{8\pi^2} \sum_f \left[\Lambda \sqrt{\Lambda^2 + M_q^2} (5M_q^2 + 2\Lambda^2 + 12U^2) + 3M_q^2 (M_q^2 + 4U^2) \ln \frac{\Lambda + \sqrt{\Lambda^2 + M_q^2}}{M_q} \right]$$

$$\begin{aligned}
& -\frac{1}{2\pi^2} \sum_f \int_0^\Lambda dp_z \left[\left(\Lambda^2 - p_z^2 + \left(\sqrt{p_z^2 + M_q^2} - U \right)^2 \right)^{\frac{3}{2}} \right. \\
& \quad \left. + \left(\Lambda^2 - p_z^2 + \left(\sqrt{p_z^2 + M_q^2} + U \right)^2 \right)^{\frac{3}{2}} \right] \\
& + \sum_f \left(\frac{M(f)^2}{4G_s} + \frac{U_f^2}{4G_p} \right) + \frac{1}{2} \frac{G_D}{G_s^3} M(u)M(d)M(s) . \tag{3.21}
\end{aligned}$$

Here, Φ_{vac} represents the contribution of vacuum. In Eq.(3.20), $[f(x)]_b^a$ means definite integral, namely $f(a) - f(b)$. Here, we defined p_{Max} and p_{min} , based on (3.16) and (3.17), explicitly,

$$\begin{aligned}
p_{Max} &\equiv \sqrt{(\mu + U)^2 - M_q^2} \quad \text{or} \quad 0 \\
p_{min} &\equiv \sqrt{(U - \mu)^2 - M_q^2} \quad \text{or} \quad 0 . \tag{3.22}
\end{aligned}$$

Thus, the thermodynamic potential can be calculated analytically, except for the second term of (3.21).

§4. Numerical results

In this section, we give numerical results. Especially, the effect of the determinant interaction on the pseudovector condensate is considered.

First, we switch off the pseudovector interaction, $G_P = 0$, namely, the pseudovector condensate being zero, $U = 0$. Then, the thermodynamic potential Φ , which represents $\Phi_{U=0}$ in this case, is written as

$$\begin{aligned}
\Phi_{U=0} &= \frac{3}{8\pi^2} \sum_f \left[\frac{1}{3} \sqrt{\mu^2 - M_q^2} (-2\mu^3 + 5\mu M_q^2) - M_q^4 \ln \frac{\mu + \sqrt{\mu^2 - M_q^2}}{M_q} \right] \theta(\mu - M_q) \\
& - \frac{3}{8\pi^2} \sum_f \left[\Lambda \sqrt{\Lambda^2 + M_q^2} (2\Lambda^2 + M_q^2) - M_q^4 \ln \frac{\Lambda + \sqrt{\Lambda^2 + M_q^2}}{M_q} \right] \\
& + \sum_f \frac{M(f)^2}{4G_s} + \frac{1}{2} \frac{G_D}{G_s^3} M(u)M(d)M(s) . \tag{4.23}
\end{aligned}$$

To determine the chiral condensates or the constituent quark masses, the gap equation is derived as

$$\frac{\partial \Phi_{U=0}}{\partial M(u)} = \frac{\partial \Phi_{U=0}}{\partial M(d)} = \frac{\partial \Phi_{U=0}}{\partial M(s)} = 0 . \tag{4.24}$$

From here, we assume isospin symmetry, namely $m_u = m_d$ and $\langle \bar{u}u \rangle = \langle \bar{d}d \rangle$. If we adopt model parameters written in Table I., the dynamical quark masses $M_{u,d} \equiv M_q$ and M_s are obtained as $M_q = 0.335$ GeV and $M_s = 0.527$ GeV, respectively. If

we neglect the determinant interaction, namely $G_D = 0$, then we have to adopt $G_S = 4.370/\Lambda^2$ instead of $3.666/\Lambda^2$ in Table II. It should be noted that the dynamical quark masses M_q and M_s do not depend on parameter G_P . Thus, it is allowed that G_P can be regarded as a free parameter in this model.

Let us assume $U \geq 0$ without loss of generality. As is well known, the chiral condensate appears in the vacuum due to the vacuum contribution. However, the pseudovector condensate does not appear in the vacuum in a realistic case. Thus, in the following parts of this section, we neglect the vacuum contribution to the pseudovector condensate for simplicity of the numerical calculation. We concentrate our attention on the appearance of the pseudovector condensate due to the particle-contribution in the quark matter only. We adopt model parameter sets in Table II. In these parameters, the pseudovector interaction strength G_P is taken as a free parameter in our consideration because this parameter could not be determined by the experimental values of a certain physical quantity. Therefore, by using these parameter sets, we investigate behavior of the pseudovector condensate in finite density quark matter. Further, to investigate the effects of the determinant interaction term \mathcal{L}_D , we include parameter sets, namely model GPnGD0 without the determinant interaction, $G_D = 0$. In these parameter sets, the dynamical quark masses M_q and M_s have almost the same values as those of the case $G_D \neq 0$.

In the following we investigate the effect of G_P . We will consider three different values of G_P : $2G_S$, $4.1G_S$ and $5G_S$, which correspond to only the appearance of the strange quark pseudovector condensate, the onset of the light quark pseudovector condensate besides the strange quark condensate, and existence of both light quark and s -quark condensates at different chemical potentials. In model GP0, namely the original 3-flavor NJL model with the determinant interaction, the chiral symmetry is broken and the non-trivial solution of the gap equation for chiral condensate or

Table I. Parameter set of 3-flavor NJL model.

Λ	G_S	G_D	$m_{u,d}$	m_s
0.6314 GeV	$3.666/\Lambda^2$	$-9.288/\Lambda^5$	0.0055 GeV	0.1357 GeV

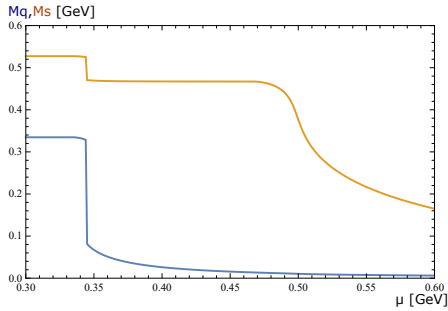


Fig. 1. Quark masses M_q (lower curve) and M_s (upper curve) are depicted as a function of chemical potential μ in model GP0.

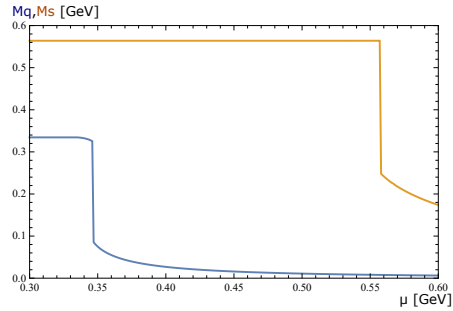


Fig. 2. Quark masses M_q (lower curve) and M_s (upper curve) are depicted as a function of chemical potential μ in model GP0GD0.

Table II. Parameter sets.

Model	Λ	G_S	G_D	G_P
GP0	0.6314GeV	$3.666/\Lambda^2$	$-9.288/\Lambda^5$	0
GP2	0.6314GeV	$3.666/\Lambda^2$	$-9.288/\Lambda^5$	$2G_S$
GP4.1	0.6314GeV	$3.666/\Lambda^2$	$-9.288/\Lambda^5$	$4.1G_S$
GP5	0.6314GeV	$3.666/\Lambda^2$	$-9.288/\Lambda^5$	$5G_S$
GP0GD0	0.6314GeV	$4.370/\Lambda^2$	0	0
GP2GD0	0.6314GeV	$4.370/\Lambda^2$	0	$2 \times 3.666/\Lambda^2$
GP4.1GD0	0.6314GeV	$4.370/\Lambda^2$	0	$4.1 \times 3.666/\Lambda^2$
GP5GD0	0.6314GeV	$4.370/\Lambda^2$	0	$5 \times 3.666/\Lambda^2$

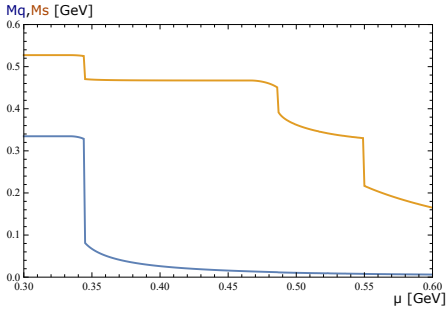


Fig. 3. Quark masses M_q (lower curve) and M_s (upper curve) are depicted as a function of chemical potential μ in model GP2.

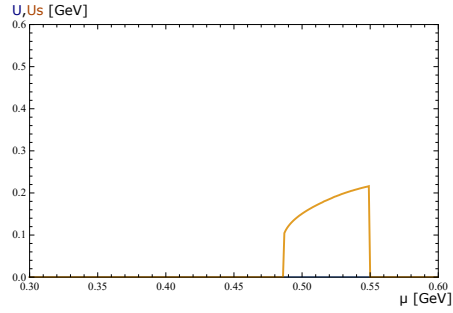


Fig. 4. Pseudovector condensate U_s is depicted as a function of chemical potential μ in model GP2.

dynamical quark mass exists in $\mu < \mu_{\text{cr}1} = 0.34$ GeV for light quarks. However, in $\mu > \mu_{\text{cr}1}$, the chiral symmetry is restored and M_q has only a small value due to the current quark mass. For strange quark, in $\mu = \mu_{\text{cr}1}$, the value of dynamical quark mass M_s decreases by the effect of the chiral restored light quarks. Also, in $\mu > \mu_{\text{cr}2} \approx 0.527$ GeV, M_s decreases monotonically. These behavior is plotted Fig.1. On the other hand, as is seen in Fig.2 for model GP0GD0 without the determinant interaction, the dynamical quark mass M_q for light quarks and M_s for the strange quark are independent each other because there is no flavor mixing caused by the determinant interaction. These results show that strange quark mass M_s is strongly affected by the effect of flavor mixing term.

In models with $G_P \neq 0$, pseudovector condensates $U_{u,d} \equiv U_q$ and U_s appear. In Figs.3 and 4, the dynamical quark masses and the pseudovector condensate U_s are depicted as a function of the quark chemical potential μ in model GP2. As is seen in Fig.3, the dynamical quark mass M_q for light quarks jumps at $\mu_{\text{cr}1}$ and for $\mu > \mu_{\text{cr}1}$ the dynamical quark mass monotonically decreases because the chiral symmetry is restored. On the other hand, for the dynamical quark mass of strange quark, first, at $\mu = \mu_{\text{cr}1}$, the mass jumps slightly. Secondly, at $\mu \approx \mu_{\text{cr}U_s1} \approx 0.486$ GeV, the dynamical quark mass decreases again. This behavior is originated from the appearance of the pseudovector condensate U_s due to strange quark. Finally, at $\mu \geq \mu_{\text{cr}U_s2} \approx 0.55$ GeV, the dynamical quark mass jumps again and the pseudovector condensate U_s

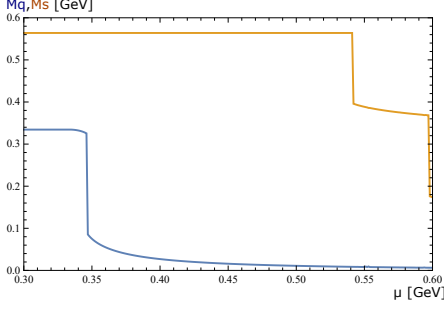


Fig. 5. Quark masses M_q (lower curve) and M_s (upper curve) are depicted as a function of chemical potential μ in model GP2GD0.

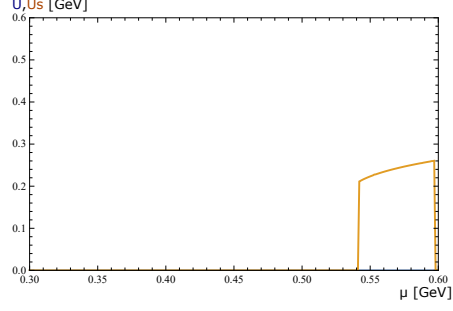


Fig. 6. Pseudovector condensate U_s is depicted as a function of chemical potential μ in model GP2GD0.

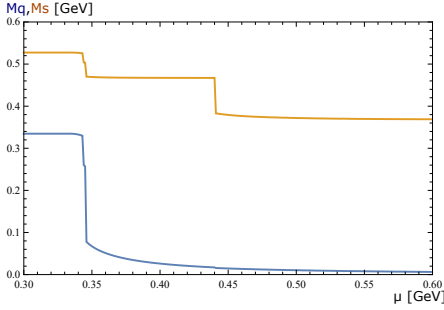


Fig. 7. Quark masses M_q (lower curve) and M_s (upper curve) are depicted as a function of chemical potential μ in model GP4.1.

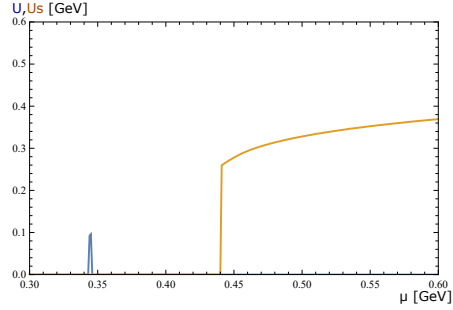


Fig. 8. Pseudovector condensates U_q (left) and U_s (right) are depicted as a function of chemical potential μ in model GP4.1.

disappears. If the pseudovector condensates do not appear, the dynamical quark masses decrease smoothly as is seen in Fig.1 due to the chiral symmetry restoration. However, when the pseudovector condensates appear, the decrease of the dynamical quark masses is suppressed. Thus, the fine structure of the behavior of dynamical quark mass as a function of the quark chemical potential, as is seen in Fig.3, appears.

In Figs.5 and 6, the dynamical quark masses and the pseudovector condensate U_s are shown as a function of μ in model GP2GD0 without the determinant interaction. The light quark mass and the strange quark mass show a rather simple behavior. Also, the pseudovector condensate U_s appears in a certain range of μ . This behavior is similar to the one of the pseudovector condensate U_q instead of U_s in the two-flavor NJL model shown in our previous paper. Further, it is shown that the critical chemical potential $\mu_{\text{cr}U_s1}$ at which the pseudovector condensate U_s for the strange quark appears is smaller than the one without the determinant interaction, namely, $\mu_{\text{cr}U_s1} \approx 0.486/0.541$ GeV in the case with/without the determinant interaction. In models GP2 and GP2GD0, only the pseudovector condensate U_s appears. Under this model parameter $G_P = 2G_S$, U_q does not appear.

Figures 7 and 8 are the same as Figs.3 and 4 except for the value of G_P , namely

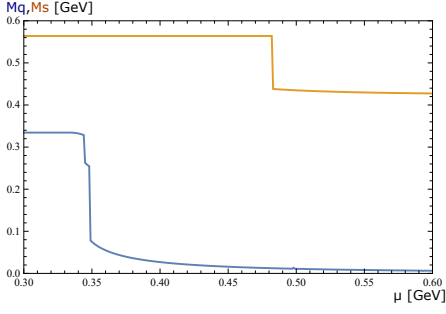


Fig. 9. Quark masses M_q (lower curve) and M_s (upper curve) are depicted as a function of chemical potential μ in model GP4.1GD0.

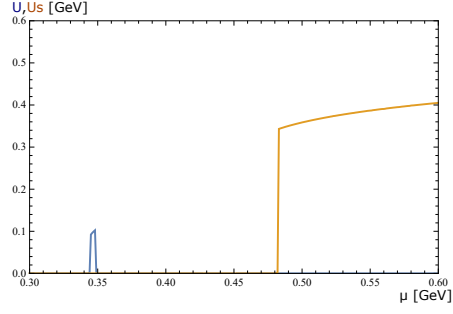


Fig. 10. Pseudovector condensates U_q (left) and U_s (right) are depicted as a function of chemical potential μ in model GP4.1GD0.

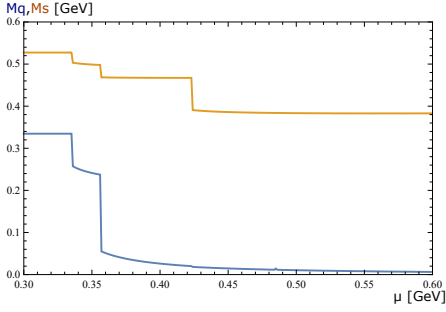


Fig. 11. Quark masses M_q (lower curve) and M_s (upper curve) are depicted as a function of chemical potential μ in model GP5.

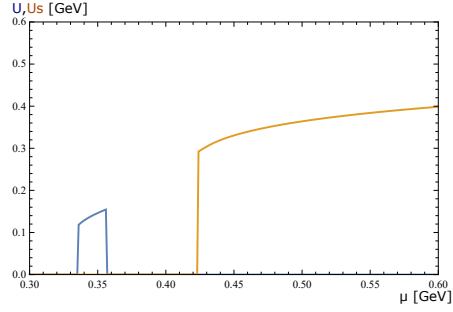


Fig. 12. Pseudovector condensates U_q (left) and U_s (right) are depicted as a function of chemical potential μ in model GP5.

$G_P = 4.1G_S$. As is seen in Fig.7, both the dynamical quark masses M_q and M_s jump slightly at $\mu_{\text{cr}U_q1} \approx 0.342$ GeV. Then, at $\mu = \mu_{\text{cr}U_q2} \approx 0.343$ GeV, the dynamical quark masses jump again. In the narrow region $\mu_{\text{cr}U_q1} < \mu < \mu_{\text{cr}U_q2}$, the pseudovector condensate for the light quarks U_q appears as is seen in Fig.8. For $\mu > \mu_{\text{cr}U_q2}$, the dynamical quark mass decreases monotonically. On the other hand, the strange quark has the finite dynamical mass about 0.48 GeV. At $\mu = \mu_{\text{cr}U_s1} \approx 0.441$ GeV, the dynamical quark mass jumps again. Simultaneously, at $\mu = \mu_{\text{cr}U_s1}$, the pseudovector condensate U_s sets in, see Fig.8.

Figures 9 and 10 are the same as Figs.5 and 6 except for the value of G_P . The behavior of the light quark mass is similar to the behavior of model GP4.1. However, the behavior of the strange quark mass is different because there is no flavor mixing. Therefore, the dynamical quark mass for strange quark is not affected by the pseudovector condensate U_q for light quark. Also, the pseudovector condensate for the light quarks is not almost affected by the determinant interaction. As in model GP2GD0, the critical chemical potential for the strange quark $\mu_{\text{cr}U_s1}$ is smaller than the one without the determinant interaction, namely, $\mu_{\text{cr}U_s1} \approx 0.441/0.482$ GeV in the case with/without the determinant interaction.

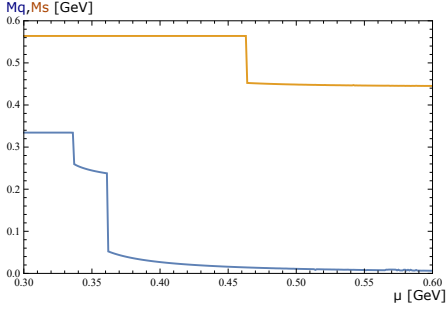


Fig. 13. Quark masses M_q (lower curve) and M_s (upper curve) are depicted as a function of chemical potential μ in model GP5GD0.

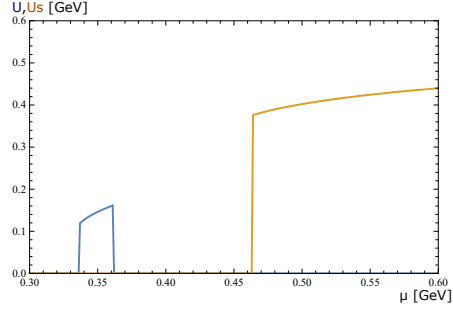


Fig. 14. Pseudovector condensate U_q (left) and U_s (right) are depicted as a function of chemical potential μ in model GP5GD0.

Figures 11 and 12 are the same as Figs.7 and 8 except for $G_P = 5G_S$. This model has a large coupling constant of the pseudovector interaction between quarks. In this model, the critical chemical potentials have the values of $\mu_{crU_q1} \approx 0.333$ GeV, $\mu_{crU_q2} \approx 0.358$ GeV and $\mu_{crU_s1} \approx 0.423$ GeV. The regions in which U_q and U_s exist are expanded, compared to model GP4.1. In this strong coupling case with $G_P = 5G_S$, the pseudovector condensate does not disappear in $\mu < \Lambda$.

Figures 13 and 14 are the same as Figs.9 and 10 except for value of G_P . Comparing Figs.12 with 14, it is seen that the pseudovector condensate for the light quarks is not almost affected by the determinant interaction. In the models of GP5 and GP5GD0, the critical chemical potential for the strange quark μ_{crU_s1} takes the value of $\mu_{crU_s1} \approx 0.423/0.463$ GeV in the case with/without the determinant interaction.

§5. Summary and concluding remarks

It has been shown that the pseudovector condensate, which leads to the quark-spin polarization as was shown in our previous paper,²⁷⁾ occurs due to the pseudovector-type four-point interaction between quarks in quark matter at zero temperature within the three-flavor NJL model. Focusing on the determinant interaction in three-flavor NJL model which leads to the quark-flavor mixing, we have investigated the effect of flavor mixing on the dynamical quark masses and the pseudovector condensates. As a result, the quantities related to the strange quark are affected by the determinant interaction, especially the behavior of the dynamical quark mass as a function of the quark chemical potential, while the quantities related to the light quarks are hardly affected. The pseudovector condensate related to the strange quark occurs at a rather small quark chemical potential compared with the case of no flavor mixing, namely, the case without the determinant interaction. The different behavior of the quark masses, which depend strongly on the presence of the determinant interaction, is the cause of this result.

Under the model parameters used in this paper, the pseudovector condensate for light quarks and one for the strange quark do not coexist. It may be necessary to

investigate the possibility of the coexistence of both the pseudovector condensates due to the light quarks and the strange quark. This is one of future problems to solve. Also, we have not explicitly calculated magnetic properties, such that spontaneous magnetization, magnetic susceptibility and so on. These are interesting future problems which are left in order to clarify the magnetic properties of high density quark matter. Further, the implication to the compact stars such as the neutron star and magnetar should be investigated by assuming the existence of the pseudovector condensate related to the light quarks and the strange quark. In this investigation, it is necessary to impose the beta equilibrium and the charge neutrality conditions. In the case with tensor-type condensate under the tensor-interaction in the NJL model,³¹⁾ the influence of the condensate for the hybrid star has been investigated under the beta equilibrium and charge neutrality conditions. In this paper, it has been also shown that the quark chemical potential in which the tensor condensate appears is slightly large compared with no beta equilibrium and charge neutrality conditions and the value of the condensate is smaller. It may be interesting to evaluate the equation of state with pseudovector condensate and to investigate the effect of it on the structure of compact star. This may be interesting future problem.

Acknowledgements

Two of the authors (M.M and Y.T.) would like to express their sincere thanks to Dr. E. Nakano for his important suggestion.

References

- 1) K. Fukushima and T. Hatsuda, *Rep. Prog. Phys.* **74**, 014001 (2011).
- 2) M. Alford, K. Rajagopal and F. Wilczek, *Nucl. Phys. B* **537**, 443 (1999).
- 3) K. Iida and G. Baym, *Phys. Rev. D* **63**, 074018 (2001).
- 4) M. G. Alford, A. Schmitt, K. Rajagopal and T. Schafer, *Rev. Mod. Phys.* **80**, 1455 (2008) and references cited therein.
- 5) L. McLerran and R. D. Pisarski, *Nucl. Phys. A* **796**, 83 (2007).
- 6) E. Nakano and T. Tatsumi, *Phys. Rev. D* **71**, 114006 (2005).
- 7) T. Tatsumi, *Phys. Lett. B* **489**, 280 (2000).
- 8) A. Iwazaki, O. Morimatsu, T. Nishikawa and M. Ohtani, *Int. J. Mod. Phys. A* **22**, 721 (2007).
- 9) E. Nakano, T. Maruyama and T. Tatsumi, *Phys. Rev. D* **68**, 105001 (2003).
- 10) T. Tatsumi, T. Maruyama and E. Nakano, *Prog. Theor. Phys. Suppl.* No. 153, 190 (2004).
- 11) H. Bohr, P. K. Panda, C. Providência and J. da Providência, *Braz. J. Phys.* **42**, 68 (2012).
- 12) H. Bohr, P. K. Panda, C. Providência and J. da Providência, *Int. J. Mod. Phys. E* **22**, 1350019 (2013).
- 13) Y. Tsue, J. da Providência, C. Providência and M. Yamamura, *Prog. Theor. Phys.* **128**, 507 (2012).
- 14) Y. Tsue, J. da Providência, C. Providência, M. Yamamura and H. Bohr, *Prog. Theor. Exp. Phys.* **2013**, Issue 10, 103D01 (2013).
- 15) Y. Tsue, J. da Providência, C. Providência, M. Yamamura and H. Bohr, *Prog. Theor. Exp. Phys.* **2015**, Issue 1, 013D02 (2015).
- 16) Y. Tsue, J. da Providência, C. Providência, M. Yamamura and H. Bohr, *Prog. Theor. Exp. Phys.* **2015**, Issue 10, 103D01 (2015).
- 17) H. Matsuoka, Y. Tsue, J. da Providência, C. Providência, M. Yamamura and H. Bohr, *Prog. Theor. Exp. Phys.* **2016**, Issue 5, 053D02 (2016).
- 18) H. Matsuoka, Y. Tsue, J. da Providência, C. Providência and M. Yamamura, *Phys. Rev.*

- D* **95**, 054025 (2017).
- 19) E. J. Ferrer, V. de la Incera, I. Portillo and M. Quiroz, *Phys. Rev. D* **89**, 085034 (2014).
 - 20) T. Maruyama and T. Tatsumi, *Phys. Rev. D* **96**, 096016 (2017).
 - 21) T. Maruyama, E. Nakano, K. Yanase and N. Yoshinaga, *Phys. Rev. D* **97**, 114014 (2018).
 - 22) Y. Nambu and G. Jona-Lasinio, *Phys. Rev.* **122**, 345 (1961), *Phys. Rev.* **124**, 246 (1961).
 - 23) S. P. Klevansky, *Rev. Mod. Phys.* **64**, 649 (1992).
 - 24) T. Hatsuda and T. Kunihiro, *Phys. Rep.* **247**, 221 (1994).
 - 25) M. Buballa, *Phys. Rep.* **407**, 205 (2005).
 - 26) S. Maedan, *Prog. Theor. Phys.* **118**, 729 (2007).
 - 27) M. Morimoto, Y. Tsue, J. da Providência, C. Providência and M. Yamamura, *Int. J. Mod. Phys. E* **27**, 1850028 (2018).
 - 28) A. K. Harding and D. Lai, *Rept. Prog. Phys.* **69**, 2631 (2006).
 - 29) M. Kobayashi and T. Maskawa, *Prog. Theor. Phys.* **44**, 1422 (1970).
 - 30) G. 't Hooft, *Phys. Rev. D* **14**, 3432 (1976). [Erratum, *ibid.* *D* **18**, 2199 (1978).]
 - 31) H. Matsuoka, Y. Tsue, J. da Providência, C. Providência and M. Yamamura, *Phys. Rev. D* **98**, 074027 (2018).